Psychoacoustic modelling of rotor noise

Antonio J. Torija,[1 a] Zhengguang Li[2], and Paruchuri Chaitanya,[3]

[1] *Acoustics Research Centre, University of Salford, Manchester, M5 4WT, United Kingdom*

[2] *Department of Architecture, Zhejiang University of Science and Technology, Hangzhou, 310023, P.R. China*

[3] *Institute of Sound and Vibration Research, University of Southampton, Southampton, SO17 1BJ, United Kingdom*

The aviation sector is rapidly evolving with more electric propulsion systems and a variety of new technologies of Vertical Take-Off and Landing (VTOL) manned and Unmanned Aerial Vehicles (UAVs). Community noise impact is one of the main barriers for the wider adoption of these new vehicles. Within the framework of a perception-driven engineering approach, this paper investigates the relationship between sound quality and first order physical parameters in rotor systems to aid design. Three case studies are considered: (i) contra-rotating vs. single rotor systems, (ii) varying blade diameter and thrust in both contra-rotating and single rotor systems, and (iii) varying rotor-rotor axial spacing in contra-rotating systems. The outcomes of a listening experiment, where participants assessed a series of sound stimuli with varying design parameters, allow a better understanding of the annoyance induced by rotor noise. Further to this, a psychoacoustic annoyance model optimised for rotor noise has been formulated. The model includes a novel psychoacoustic function to account for the perceptual effect of impulsiveness. The significance of the proposed model lies in the quantification of the effects of psychoacoustic factors such as loudness as dominant factor, and also tonality, high frequency content, temporal fluctuations, and impulsiveness on rotor noise annoyance.

[a] A.J.TorijaMartinez@salford.ac.uk

I. INTRODUCTION

With the forecast of a substantial expansion of the Unmanned Aerial Vehicles (UAV) sector, the consequent noise generated might lead to a significant problem for public acceptance. The optimisation of UAV designs for minor noise impact on communities requires a complete understanding of sound generation mechanisms of UAV rotors. To date, there is a comprehensive literature on rotorcraft noise, including noise prediction (Brentner and Farassat, 1994; Brès *et al.*, 2004; Romani and Casalino, 2019) and annoyance ratings (Boucher *et al.*; Fields and Powell, 1987; Gjestland, 1994). However, due to the operating conditions of rotorcraft, i.e., high Mach numbers in the transonic regime, this literature might not be of direct application to UAV rotors. During the last few years, researchers have investigated the aeroacoustics of UAV rotors, i.e. with low Reynolds number and low Mach number (Gojon *et al.*, 2021). Recent research has shown that far-field noise of UAV rotors is mainly characterised by prominent tones at the Blade Passing Frequency (BPF) and its harmonics, and broadband noise at mid and high frequencies (Zawodny *et al.*, 2016; Torija, 2019).

Gojon et al. (Gojon *et al.*, 2021) conducted an experimental investigation for the acoustic characterization of low Reynolds number isolated rotors. The authors found that for all rotors examined, the far-field frequency spectra were dominated by tonal noise (BPF and its harmonics) and broadband trailing edge noise. Changes in directivities of BPF and overall sound pressure level (OASPL) were observed as a function of rotation speed and number of blades, assumed to be due to phase cancellation of thickness and loading noise sources. Gojon et al. (Gojon *et al.*, 2021) also discussed the balance between tonal and broadband noise contributions as a function of blade number, i.e., an increase in blade number led to a decrease in BPF amplitude but an increase in broadband noise. Zawodny and Boyd (Zawodny and Boyd, 2019) and Whelchel et al. (Whelchel *et al.*, 2020) studied the rotor-airframe interaction for a variety of simplified configurations. More complex configurations like multi-rotors have been investigated by Intaratep et al. (Intaratep *et al.*, 2016) and

Tinney and Sirohi (Tinney and Sirohi, 2018). Tinney and Sirohi (Tinney and Sirohi, 2018) investigated the effect of the change in blade length on noise emissions in multi-rotors, and also observed how small tip-to-tip distances between rotor blades result in a significant increase in noise emissions due to blade interaction effects.

For the specific case of contra-rotating systems, Luan et al. (Luan *et al.*, 2019) found a strong relationship between the axial rotor spacing and OASPL, with a general trend indicating that OASPL decreases with increase in axial spacing. Torija et al. (Torija *et al.*, 2021) suggested an optimal rotor axial separation distance (relative to the blade diameter) between 0.2 and 0.4. Chaitanya et al. (Paruchuri *et al.*, 2021) discussed the reason behind this optimum and attributed it to an optimum balance between the various dominant sources. The potential field interactions were shown to dominate overall noise at separation distances smaller than the optimum distance, while the noise due to tip vortex interaction is dominant for distances greater than the optimum value. Analytical predictions were also performed by Chaitanya et al.(Paruchuri *et al.*, 2021) to validate their hypothesis. McKay et al. (McKay *et al.*, 2019) carried out an experimental investigation on noise of contra-rotating systems with varying rotor axial spacing, blade diameter, and blade number. The authors found significant differences in OASPL depending on the specific configuration. The main source of noise identified was potential field interaction tones. It was observed that potential field interaction tones are about 20 dB higher than rotor alone tones at 45 degrees below the contra-rotating system (which is a typical ground observer location with a hovering UAV).

However, hitherto, there is not a comprehensive investigation to connect sound quality directly to design parameters of rotary systems. Gwak et al. (Gwak *et al.*, 2020) investigated the Sound Quality Metrics (SQMs) influencing noise annoyance of UAVs. The authors found that the SQMs loudness, sharpness and fluctuation strength are significant factors influencing the annoyance reported for the UAV vehicles tested. Gwak et al.'s (Gwak *et al.*, 2020) research is based on three off the shelf multicopters, and therefore does not provide a direct link between SQMs and varying design configurations. Torija et al. (Torija *et al.*, 2021) carried out an analysis based on a series of SQMs and psychoacoustic annoyance (PA) models to define the optimal rotor axial separation distance in contra-rotating systems. These authors investigated the value of several SQMs and PA models (More, 2011; Zwicker and Fastl, 2013; Di *et al.*, 2016) as a function of rotors axial spacing, and linked them to the different sound generation mechanisms.

SQMs are able to provide a very accurate representation of how the human auditory system response to different sound features. For instance, loudness and sharpness metrics account for the perceived sound intensity and content of high frequency noise respectively. The tonality metric describes how spectral irregularities or discrete tones are perceived. Other SQMs such as fluctuation strength and roughness account for the perception of slow and rapid fluctuations of the sounds level respectively; and impulsiveness describes the perception of short and sudden changes in the sound level (see Boucher et al. (Boucher *et al.*, 2019) and Torija et al. (Torija *et al.*, 2021) for further details). A complete understanding on how different design configurations influence the resulting sound quality allows a perception-influenced development of rotary systems, with the potential benefits of more efficient designs to reduce noise impact on communities (Torija and Clark, 2021).

This paper investigates the relationships between primary order design parameters of rotary systems and noise perception. Noise perception is assessed as a function of both existing SQMs and annoyance reported by participants to a comprehensive listening experiment. The specific design parameters investigated are:

- Contra-rotating vs. single rotor systems (for the same thrust).
- Different blade diameters and thrust (in contra-rotating and single rotor systems).
- Different rotor axial spacing in contra-rotating systems (with varying blade diameters).

Based on all the data gathered, i.e., participants responses to the series of stimuli encompassing different design parameters, a PA model optimised for rotor noise is formulated and analysed.

One of the major contributions of this paper is the understanding of how varying design parameters in rotary systems affect SQMs and overall perceived annoyance. This allows to update and enhance psychoacoustic annoyance models to account for the main psychoacoustic features of rotor noise. Although the aeroacoustics of single and contra-rotating systems (and primary design parameters) have been widely investigated, this paper advances at carrying out a comprehensive analysis of the relationship between physical parameters and perceptual outcomes (e.g., noise annoyance). A new psychoacoustic annoyance model has also been formulated (with a curve fitting procedure) to account for the perceptual effects of impulsiveness, which might be crucial for new rotorcraft vehicles, including multiple rotors configurations and VTOL transition maneuvers.

This paper is structured as follows: Section II describes the experimental setup for acoustic measurements; Section III describes the development of the psychoacoustic experiment and the data analysis; Section IV presents and discusses the experimental results and PA model, and are followed by the main conclusions of this work in Section V.

II. EXPERIMENTAL SET-UP FOR DATA MEASUREMENT

An overlapping rotor test rig designed and manufactured at the University of Southampton (Brazinskas *et al.*, 2016) was used to gather the experimental data for this research. This test rig was assembled with two FOXTECH W61-35 brushless DC (BLDC) (16 poles) 700W motors mounted on a carbon fibre beam. The test rig was operated in two modes, with only a rotor operating (i.e., single rotation) and with two co-axial rotors operating. Commercially available T-Motor 14 inch, 16 inch and 18 inch rotor blades were used both in isolation and also in a co-axial contra-rotating configuration. BLDC motors were controlled with two Maytech 40A-OPTO speed controllers, and

Rotations Per Minute were measured with Two Hyperion HP-EM2-TACHBL sensors (see Torija et al. (Torija *et al.*, 2021) for further details).

The overlapping rig allowed manipulation of the rotary system in rotor axial separation distance z/D (with D as the rotor diameter). Overall, sixteen z/D positions were measured: 0.05, 0.075, 0.1, 0.125, 0.15, 0.175, 0.2, 0.25, 0.3, 0.35, 0.4, 0.45, 0.5, 0.6, 0.8 and 1.0. Note that all measurements were taken with the lower rotor plane was at least three rotor diameters away from the ground with anechoic wedges beneath. In this research, only z/D positions 0.05, 0.1, 0.2, 0.4, 0.6 and 1.0 are considered for the listening experiment and further analysis.

The combined thrust of the contra-rotating system was varied from 2 to 20N in steps of 2N. In additions, for comparison the single-rotor propulsion system was varied from 1 to 10N in steps of 1N. In this research, only data measured at 6N and 10N (single rotation), and 6N, 10N and 16N (contra-rotation) is considered for the listening experiment and further analysis.

III. DEVELOPMENT OF PSYCHOACOUSTIC EXPERIMENT AND DATA ANALYSIS

A. Sound recording

Sound samples for the listening experiment and psychoacoustic analysis were extracted from a series of far-field noise measurements made for the different configurations described in section II. The far-field measurements were carried out at the Institute of Sound and Vibration Research's open-jet wind tunnel facility, with the overlapping rotor test rig placed within an anechoic chamber (dimensions = 8 m × 8 m × 8 m, and cut-off frequency of 80 Hz).

An array of 10 ½ in. condenser microphones (B&K type 4189) was used for the far-field measurements (see Figure 1). This array of microphones was located at a constant radial distance of

2.5 m from the centre of the propellers. The microphones were placed at emission angles of between about 10 degrees and 100 degrees, measured relative to the bottom rotor. Note that, only data measured at emission angles 10 degrees and 85 degrees was considered for the listening experiment and psychoacoustic analysis. Ten degrees and 85 degrees are roughly the azimuthal angles with maximum and minimum emission respectively for potential field interaction tones (McKay *et al.*, 2019; Torija *et al.*, 2021).

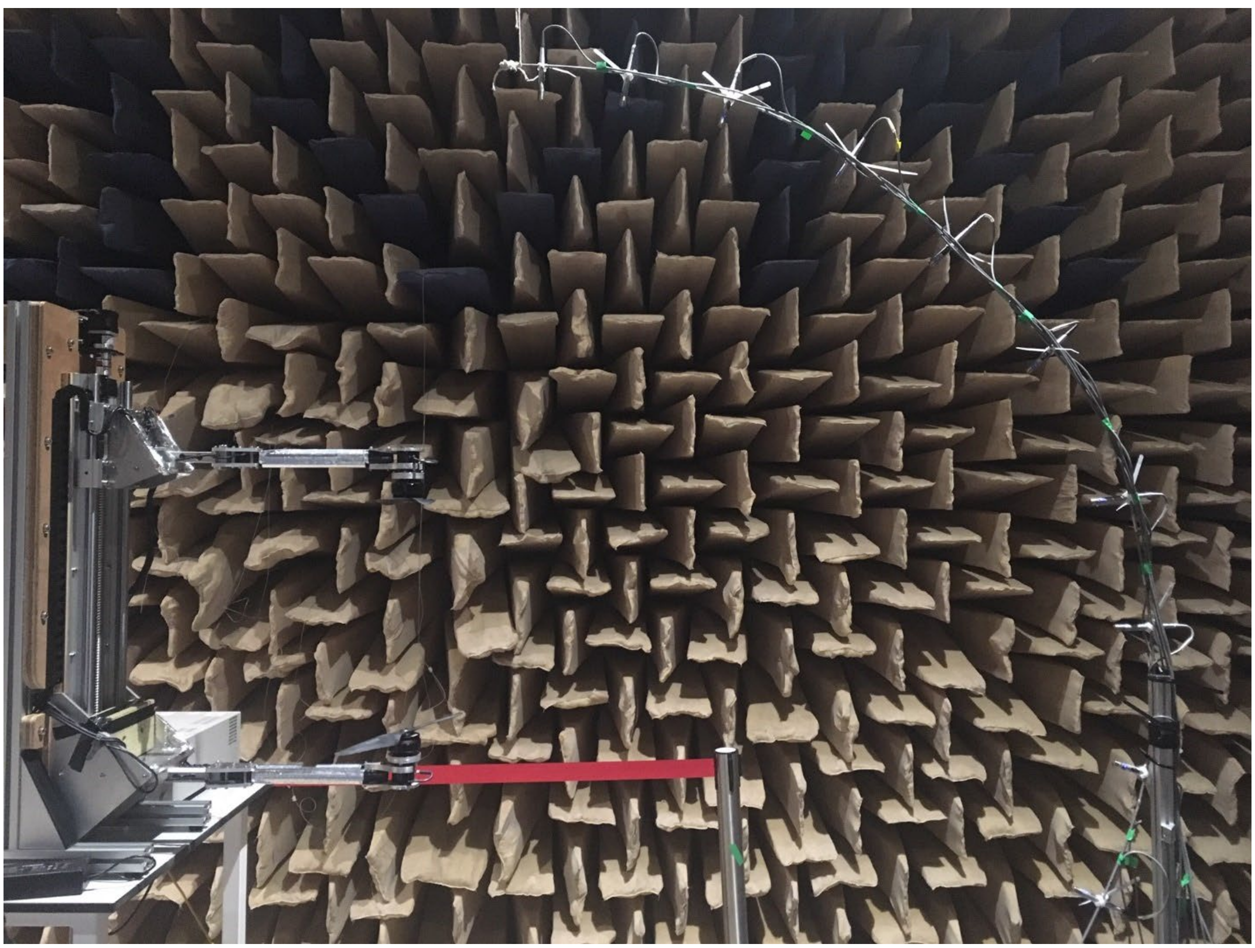

Figure 1. Experimental setup. (color online)

These far-field noise measurements were carried out for 10 s duration at a sampling frequency of 50 kHz. The frequency spectra were obtained with a window size of 1024 data points, with corresponds to a frequency resolution of 48.83 Hz and a Bandwidth-Time product of about 500. This is considered sufficient to ensure negligible variance in the spectra estimated at this frequency resolution.

B. Sound stimuli

Ninety-two stimuli, including 84 test stimuli, 7 master scaling stimuli and 1 reference stimulus, were used in the listening experiment. As described in section II.A, these sound stimuli were selected from the far-field noise database recorded, to account for a wide range of design parameters in a rotary system. This was deemed to be essential to develop a psychoacoustic annoyance model able to account for the perceptual effects of the major features of rotor noise. The list of sound stimuli used in the listening experiment are summarized in Table I.

Table I. Summary of sound stimuli used in the listening experiment.

Stimuli	Rotary System	Thrust (N)	Blade diameter (inch)	Axial spacing (z/D)	Emission angles (degrees)	Numbers of stimuli
Reference stimulus	Contra-rotating	16	16	0.15	100	1
Master scaling stimuli	Contra-rotating	10	16	0.075	20	7*
Test stimuli in Part 1	Contra-rotating	6 10	16	0.05, 0.1, 0.2, 0.4, 0.6, 1	10 85	24
	Single-rotor	6 10	14 16 18	-	10 85	12
Test stimuli in Part 2	Contra-rotating	16	16	0.05, 0.1, 0.2, 0.4, 0.6, 1	10 85	12
	Contra-rotating	16	14 16 18	0.05, 0.1, 0.2, 0.4, 0.6, 1	10 85	36

*These 7 stimuli were from the same sound recording but with different sound levels after adjustment in amplitude (to derive a master-scale, see Section III.F).

The duration of all stimuli was 3 s. This stimuli length was carefully selected to be long enough for the participants to be able to decide and report perceived annoyance while minimizing participant's fatigue (Torija and Flindell, 2015). Both to increase the realism of the scenarios presented (i.e., vehicle hovering) and minimise the risk of sound exposure, the sound level of all the stimuli were normalised to the level at the position of 50 m from the centre of the propellers, according to the sound propagation law of a point source. The target sound level (L_{Aeq}) of the reference stimulus was set at 51.8dBA. This specific L_{Aeq} was chosen as it is the median (L_{Aeq}) value of all the test sounds used in the subjective experiment. The reference stimulus was selected because it has an 'average' loudness (considering all the test sounds), and it does have any significantly perceivable psychoacoustic feature (i.e., tonality, amplitude modulation, roughness, etc.). The 7 master scaling stimuli were generated from the same stimulus by modifying its sound level (L_{Aeq}) to 40.1dBA ~ 70.1dBA, in increments of 5dB. These 7 master scaling stimuli covered approximately the whole range of L_{Aeq} of all the test stimuli used, which ranged from 39dBA to 68.9dBA. The sound used to synthesise the 7 master scaling stimuli was dominated by the present of potential field interaction tones, as the main sound generation mechanisms in contra-rotating systems with rotors closely spaced (Paruchuri *et al.*, 2021; Torija *et al.*, 2021). A clearly dominant acoustic feature with sound levels varying widely, to cover the whole range of test sounds, allowed the derivation of a linear master scale as described in section III.F.

C. Experimental setup

The hardware setup used for the listening experiment consisted of a powerful desktop computer (Intel Core i7-2600 CPU @3.40 GHz, 16.0 GB RAM, 64-bit Windows 10 Operating System) with a USB DAC/headphone amplifier (Audioquest, DragonFly Cobalt v1.0) and a pair of open back headphones (Audio-Technica, ATH-M70x). The listening tests were carried out in a very quiet environment (i.e., a lab room of Zhejiang University of Science and Technology, with the background sound level of 21.6 dBA), with no interference from outside in order to avoid distractions.

The test was entirely automated via a bespoke MATLAB code. The volume level on the desktop was always set to maximum, with MATLAB controlling the playback volume to ensure consistency.

The headphone reproduction was calibrated in sound pressure level using an artificial head (HEAD acoustics GmbH, HMS IV.0) to the corresponding target sound levels, without altering neither temporal nor spectral characteristics.

D. Participants

The listening tests were undertaken by 33 healthy participants (17 males and 16 females) aged between 20 and 23 years old (mean age = 21.2, standard deviation = 0.8) who were recruited by advertisement within Zhejiang University of Science and Technology. A thank you gift of ¥50 for taking part was used to incentivize participation in the listening tests. Prior to participating in the listening test, each participant was required to confirm normal hearing ability and asked to fill out a consent form.

Responses from 4 participants were discarded due to severe inconsistencies in their responses. Therefore, the responses of perceived annoyance reported by these 4 participants were not considered in the psychoacoustic analysis carried out. Finally, responses from 29 participants (14 males and 15 females) aged between 20 and 23 years old (mean age = 21.1, standard deviation = 0.9) were analysed in this paper.

E. Experimental procedure

The listening experiment started with the participants being presented 7 sounds to derive a master scale. As described above, these sounds were the same sound sample (see Table I for details) with 7 different sound levels. The goal of deriving a master scale is to scale and calibrate the scales used by different participants to a common master scale (De Coensel *et al.*, 2007).

After the master scale part was finished, the listening experiment involved a series of assessment task groups, where the participants reported their perception of noise annoyance induced by the sounds they heard, using a relative-number magnitude estimation scale. The relative magnitude estimation method (Huang and Griffin, 2014) was selected for reporting the perceived noise annoyance as it provides outcomes in a continuous scale, thus simplifying the derivation of the psychoacoustic annoyance model. The participants were asked to rate the perceived noise annoyance of each test sound numerically against a defined reference stimulus which was given an arbitrary rating of 100.

In order to reduce participant's fatigue, the listening experiment was divided into two parts. In part 1, the 36 stimuli (see Table I) were randomly allocated into 9 groups. In part 2, there were 48 stimuli (see Table I) which were randomly grouped into 12 groups. In each group, 5 stimuli were presented, including 1 reference stimulus and 4 test stimuli. The reference stimulus was the same for all groups, and it was presented in first place. After listening to the reference stimulus, the 4 test stimuli randomly selected were presented sequentially to the participants, with a gap of 2s in between stimulus. The participants were required to type their responses after they have heard each test stimulus. They were asked to rate numerically each test stimulus, so that the numerical difference between such stimulus and the reference stimulus (allocated noise annoyance rating of 100) reflected the perceived difference in annoyance. Note that no restriction on number values was indicated to the participants. During the assessment process, the participants were allowed to listen to each stimulus as many times as they required, and change their response until the final assessment was decided. Once a given group of stimuli was rated, the participant continued with another group until all test stimuli were rated. The duration of the whole listening experiment, including master scaling phase, part 1 and part 2 was about 30 min.

F. Master scaling

The measurement of noise-induced annoyance is always a contextually based dynamic process (Stallen, 1999). Different participants are likely to give different magnitude estimates of noise annoyance to the same stimulus, according to their own scaling context. In order to address this issue, 7 reference stimuli with varying sound level were presented to the participants to help them define their own scaling context. The reported annoyance for these reference stimuli was used to control for the individual participants' choice-of-number behaviour in scaling the test sounds. Following Berglund (Berglund, 2013), each individual participant's annoyance scale was calibrated with the reference to a common master scale.

According to De Coensel et al. (De Coensel *et al.*, 2007), individual's response to noise annoyance and the sound level of the stimuli fit according to Equation 1.

$$R = aL_p + b \qquad \text{(Equation 1)}$$

Where R is the reported annoyance, L_p is the sound level of the stimulus, and a and b are constants which are different for each participant, and therefore characterize their individual's scaling context. Note that the choice of the psychophysical function to build the common master scale (Equation 1) was based on previous research where noise annoyance values were scaled in a similar manner (De Coensel *et al.*, 2007).

The response to the 7 master scaling stimuli in this listening experiment were used to build each participant's annoyance scaling, according to Equation 1. The common master scale was built based on the average value of noise annoyance reported by all valid participants (i.e., after discarding the responses of participants with severe inconsistencies in their responses, see section III.D). By the aid of the reference to the common master scale, each individual participant's annoyance scale was calibrated using Equation 2.

$$R_i = \frac{a_i(R_0 - b_0)}{a_0} + b_i \quad \text{(Equation 2)}$$

Where R_i and R_0 are the reported annoyance to a stimulus in the scaling of participant i and in the common master scaling respectively, a_i and b_i are the constants characterizing individual's scaling, a_0 and b_0 are the constants characterising the common master scaling.

G. Data analysis

A threshold of correlation coefficient between the reported annoyance and L_{Aeq} for the master scaling stimuli was set for the participants' responses to be considered for the psychoacoustic analysis. As indicated above, 4 participants' data were discarded due to the low correlation coefficient (R^2 was lower than 0.6) between reported annoyance and L_{Aeq} for the 7 stimuli used in the master scaling part. The mean of all 29 valid participants' response was calculated as the final annoyance of each stimulus. The SQMs [including loudness in sone, sharpness in acum, fluctuation strength in vacil, roughness in asper, impulsiveness in Impulsiveness Units (IU), and tonality in Tonality Units (TU)] of all sound samples were calculated with ArtemiS software (HEAD acoustics GmbH). For further details about the specific methods implemented, see Torija et al. (Torija *et al.*, 2021) As recommended in the literature (Zwicker and Fastl, 2013), the 5th percentile of each SQM was used for the psychoacoustic analysis. As the sound stimuli were constant in amplitude, it was assumed that the findings of the psychoacoustic analysis are non-dependent of the given statistical parameter used as output of the SQM. The first 0.5 s of each sound stimulus were ignored in the calculation of the 5th percentile of each SQM, in order to avoid the transient effect of the digital filters implemented in the algorithms to calculate the SQMs.

All the statistical analyses, presented in section IV, were carried out with the statistical package IBM SPSS Statistics 25.

IV. RESULTS AND DISCUSSION

A. Contra-rotation vs. single rotor

The contra-rotating and single rotor systems were compared in terms of reported annoyance and value of SQMs. The 16 in. blade diameter configuration was selected, and comparisons were made for the 6 N and 10 N thrust settings and 10 degrees and 85 degrees emission angles. For each thrust setting and emission angle, seven cases were considered: i.e., six rotor-rotor axial spacings (z/D = 0.05, 0.1, 0.2, 0.4, 0.6, 1.0) and single rotor configuration.

An Independent-Samples Mann-Whitney U Test, carried out for the configurations and cases described above, showed that there are statistically significant differences ($p < 0.05$) between the contra-rotating and single rotor systems in terms of reported annoyance ($p = 0.024$), Loudness ($p = 0.029$), Roughness ($p = 0.042$) and Fluctuation Strength ($p = 0.019$). Even though the same thrust is generated, the loudness of the single rotor is significantly lower than the loudness of the contra-rotating system (even for the psychoacoustic optimal axial spacing (Torija *et al.*, 2021)). Rotor-rotor interaction also leads to higher values of Roughness and Fluctuation Strength for the contra-rotating system, compared to the single rotor. Roughness has significant values at higher rotor-rotor axial spacings (i.e., z/D = 0.6, 1.0), while Fluctuation Strength has the highest values either at reduced rotor-rotor axial spacings (z/D = 0.05, 0.1) or large rotor-rotor axial spacings (i.e., z/D = 0.6, 1.0). This has been previously identified by Torija et al. (Torija *et al.*, 2021) and attributed to the enhancement of turbulence-rotor interaction noise at larger rotor-rotor axial spacing. Similarly, at lower rotor-rotor axial spacing distances the dominant noise generating mechanism is due to the potential field interactions (McKay *et al.*, 2019; Torija *et al.*, 2021). Note that one of the main perceptual differences when listening to contra-rotating sounds, as compared to single rotors, is the beating sound (i.e., a sound with low frequency amplitude modulation). The annoyance reported for the single rotor case is 48% (6 N / 10 degrees), 24% (6 N / 85 degrees), 57% (10 N / 10 degrees) and

48% (10 N / 85 degrees) lower than the annoyance reported for the rotor-rotor axial spacing z/D = 0.2 (psychoacoustic optimal axial spacing (Torija *et al.*, 2021)).

In Figure 2, it can be seen that the differences in reported annoyance (i.e., inter-individual average value for each test sound) and Loudness between the contra-rotating and single rotor systems are higher at 10 degrees (i.e. emission angle with high amplitude of potential field interaction tones (McKay *et al.*, 2019; Torija *et al.*, 2021)) than at 85 degrees, where the emission of rotor alone tones dominate.

It should be noted that plots for Roughness and Fluctuation Strength have not been included in Figure 2, as the association between these two SQMs and reported annoyance is influenced by Loudness (as a confounding factor). See section IV.D for further details.

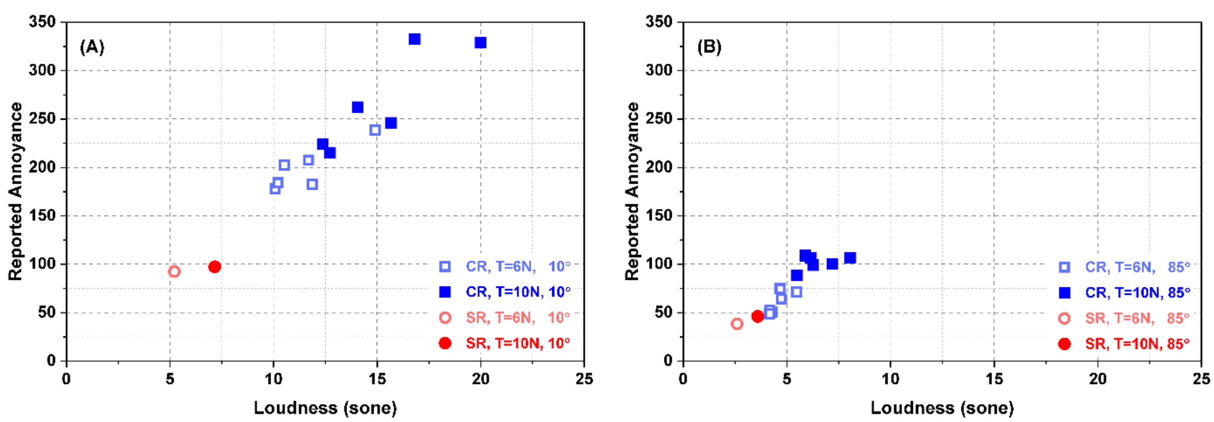

Figure 2. Reported annoyance (i.e., inter-individual average value for each test sound) vs. Loudness, for emission angle of 10 degrees (A) and 85 degrees (B). Configuration with 16 in blade diameter, and thrust setting of 6 N and 10 N. (color online)

B. Psychoacoustic metrics and annoyance vs. rotor spacing

The changes in SQMs with varying rotor-rotor axial spacing (z/D) in the contra-rotating system was investigated. Figure 3 (A) to Figure 3 (F) displays the values of Loudness, Sharpness, Aures Tonality, Fluctuation Strength, Roughness and Impulsivenes for rotor-rotor axial spacings (z/D) 0.05, 0.1, 0.2, 0.4, 0.6 and 1.0. Figure 3 shows the mean values and standard deviations bars for the data including 14 in, 16 in and 18 in blade diameter; 6 N, 10 N and 16 N thrust settings; and emission angles 10 degrees and 85 degrees.

As described in Torija et al. (Torija *et al.*, 2021), at reduced rotor-rotor axial spacing the dominant noise source in contra-rotating systems are potential field interaction tones. As the axial spacing between the rotors increases, the magnitude of such potential field interaction tones becomes smaller, and consequently the overall Loudness (Figure 3 (A)) and Aures Tonality (Figure 3 (C)) is significantly reduced, reaching minimum values at about z/D = 0.2 – 0.4. This decrease in the amplitude of potential field interaction tones has two other effects: the beating effects (or low frequency amplitude modulation) due to the interaction between rotors diminishes (see Figure 3 (D) for a reduction of Fluctuation Strength until z/d = 0.4 as rotor-rotor axial spacing increases); with a lesser amplitude of potential field interaction tones (i.e., dominant noise source) at about z/D = 0.2 – 0.4, the contribution of high frequency tonal and broadband components becomes more important, and therefore an increase in Sharpness is observed (see Figure 3 (B)). At larger rotor-rotor axial spacing the dominant noise source in contra-rotating systems are enhanced turbulence-rotor blade interactions. This is illustrated by the significant increase of both Roughness (Figure 3 (E)) and Impulsiveness (Figure 3 (F)) as the axial spacing between rotors increases. These two SQMs are strongly linked to each other (Krishnamurthy *et al.*, 2018) and have been found to be able to account for the unsteadiness in rotor noise. (Torija *et al.*, 2021) This added unsteady turbulence-rotor blade interaction noise causes an increase in Loudness as the rotors move apart from each other.

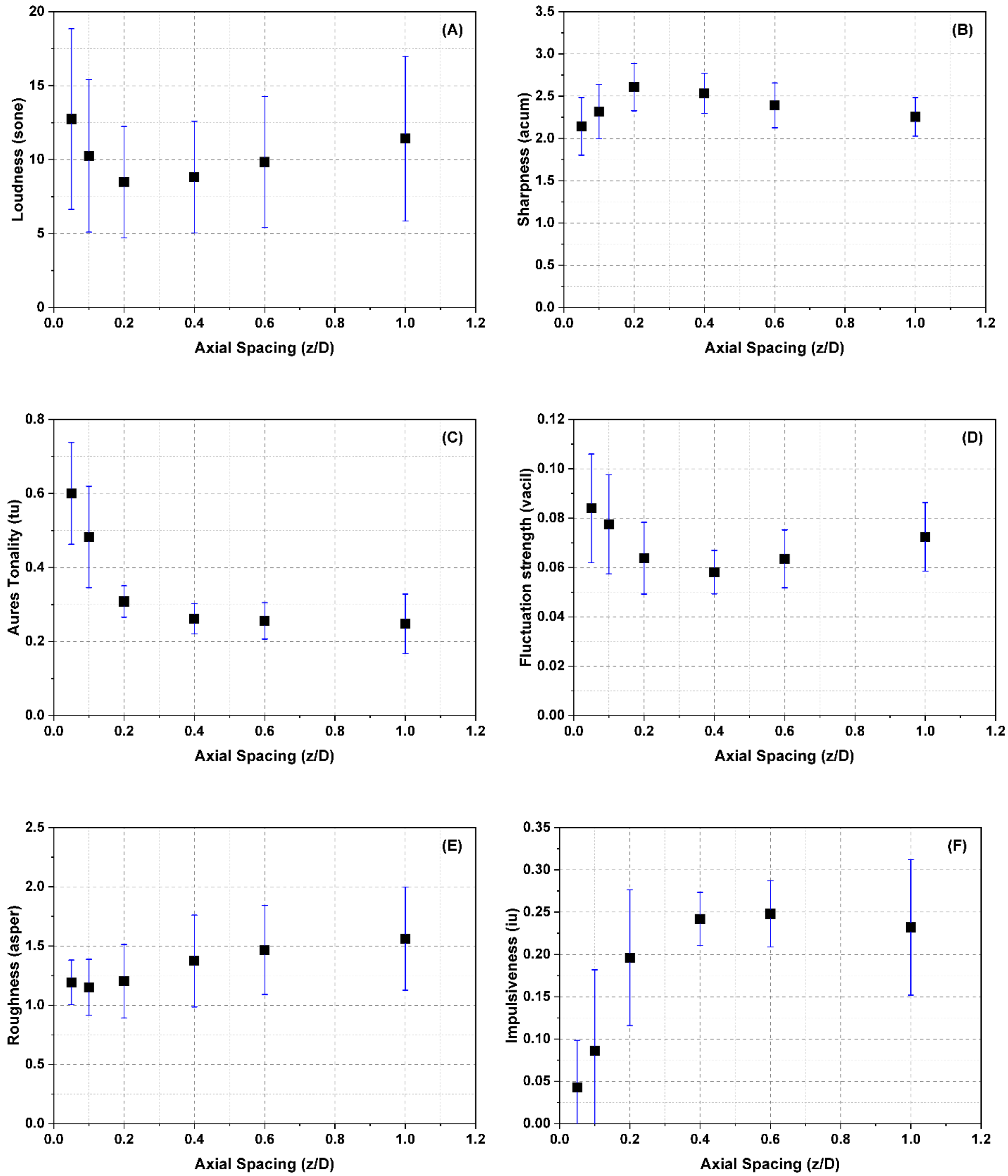

Figure 3. The 5th percentiles of Loudness (A), Sharpness (B), Aures Tonality (C), Fluctuation Strength (D), Roughness (E) and Impulsiveness (F) as a function of rotor-rotor axial spacing (z/D). Standard

deviation bars accounts for varying configurations: 14 in, 16 in and 18 in blade diameter; 6 N, 10 N and 16 N thrust settings; and emission angles 10 degrees and 85 degrees. (color online)

Figure 4 shows the inter-individual average values (and standard deviation bars accounting for varying configurations: 14 in, 16 in and 18 in blade diameter; 6 N, 10 N and 16 N thrust settings; and emission angles 10 degrees and 85 degrees) of the reported annoyance as a function of rotor-rotor axial spacing (z/D). As can be seen in Figure 4, the participants of the subjective experiment found the sound samples at an axial spacing z/D = 0.2 as the less annoying. The presence of potential field interaction tones at reduced rotor-rotor axial spacing, and unsteady turbulence-rotor blade interaction at larger spacings, seemed to be picked up by participants responses. The trend of reported annoyance as a function of axial spacing between rotors almost matches the Loudness vs. axial spacing pattern. This seems to suggest that the participants responses were mainly driven by Loudness, although further analysis is needed (see Section IV. D). Exploring Figure 3, it can be seen that participants' responses might somehow be influenced the significant reduction of Aures Tonality (after z/D = 0.2), and the Fluctuation Strength vs. axial spacing pattern (with the lowest values at z/D = 0.2-0.4). This might suggest that Loudness is the main contributor for the reported annoyance for the contra-rotating system investigated, although the influence of Tonality and low frequency amplitude modulation (due to beating effects between rotors) should also be considered. However, the specific contribution of Tonality and Fluctuation Strength to reported annoyance should be interpreted with caution as explained in section IV.D.

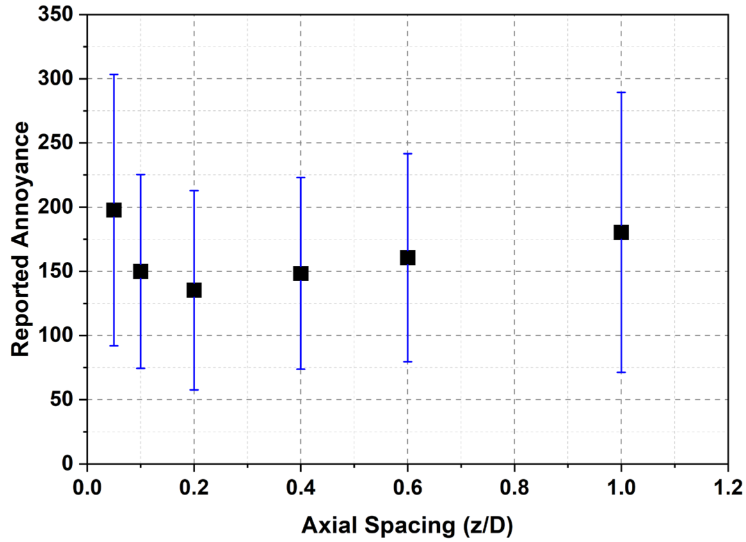

Figure 4. Reported annoyance as a function of rotor-rotor axial spacing. Standard deviation bars accounts for varying configurations: 14 in, 16 in and 18 in blade diameter; 6 N, 10 N and 16 N thrust settings; and emission angles 10 degrees and 85 degrees. (color online)

C. Psychoacoustic metrics and annoyance vs. blade diameter

Figure 5 shows the changes in Loudness and reported annoyance (i.e., inter-individual average values per test sound) for the three blade diameters (i.e., 14 in, 16 in, and 18 in) considered in this research for the single rotor configuration. Results are shown for thrust settings of 6 N and 10 N, and for emission angles of 10 degrees and 85 degrees. In general, as seen in Figure 5, reported annoyance diminishes with the increase of blade diameter. This is in line with the decrease of Loudness with blade diameter. Figure 5 shows a reduction of Loudness from 14 in blade diameter to 16-18 in blade diameters. Table II also displays the average value (accounting for data for thrust settings of 6 N and 10 N, and for emission angles of 10 degrees and 85 degrees) for the SQMs Sharpness, Aures Tonality, Fluctuation Strength, Roughness and Impulsiveness as a function of blade diameter. As the blade diameter increases from 14 in to 18 in, there is a slight reduction of Sharpness and an important decrease of Aures Tonality. The reduction of Loudness seems to drive the responses of the participants for lower reported annoyance as rotor blade diameter increases.

For a given thrust, an increase in blade diameter leads to a reduction of blade loading. As stated by Tinney and Sarohi (Tinney and Sirohi, 2018), an increase of rotor blade diameter can ensure the generation of the same thrust levels with lower rotational speed, leading this to an important reduction of thickness and loading noise. That reduction in the rotational speed of the single rotor system causes a displacement of the BPF (and its harmonics) towards the low frequency region, with the consequent reduction in Sharpness and Aures Tonality. At the same time, as shown in Table II, the increase in rotor blade diameters leads to an increase in Roughness and Impulsiveness, which might indicate an increase in broadband noise due to interaction of boundary layer with blade trailing edge and the interaction of turbulent wake with neighboring propeller blade. Larger diameter propeller blades have larger chord and hence the boundary layer thickness increases which results in increases in broadband noise. Chaitanya et. al. (Paruchuri *et al.*, 2021) argues that for a single rotor, the radiated acoustic power varies as $\boldsymbol{N}^{5.5}\boldsymbol{D}^{3}$, where $\boldsymbol{N}$ is the rotational speed and $\boldsymbol{D}$ is the diamater of the propeller. The total noise therefore follows a thrust scaling law of $\boldsymbol{T}^{2.75}$ and velocity scaling law of $\boldsymbol{U}^{5.5}$, which is identical to the scaling law characteristics of aerofoil leading edge noise. With the increase in propeller diameter, to maintain the same thrust the rotational speed ($\boldsymbol{N}$) needs to be reduced, which results in reduction of radiated noise following scaling law $\boldsymbol{N}^{5.5}\boldsymbol{D}^{3}$. With larger diameter propellers, the BPF occurs at lower frequencies and hence this results in lower sharpness compared with smaller diameter propellers. It is worth noting here that in this scaling with rotational speed, $\boldsymbol{N}$ is predominant compared to diameter $\boldsymbol{D}$. The reason behind this may requires further work.

For the case of a thrust setting of 10 N at the emission angle 10 degrees, the value of reported annoyance for the 16 in blade diameter is lower than for the 18 in blade diameter. This might be attributable to the slightly lower Loudness of the 16 in blade diameter, compared to the Loudness of the 18 in blade diameter.

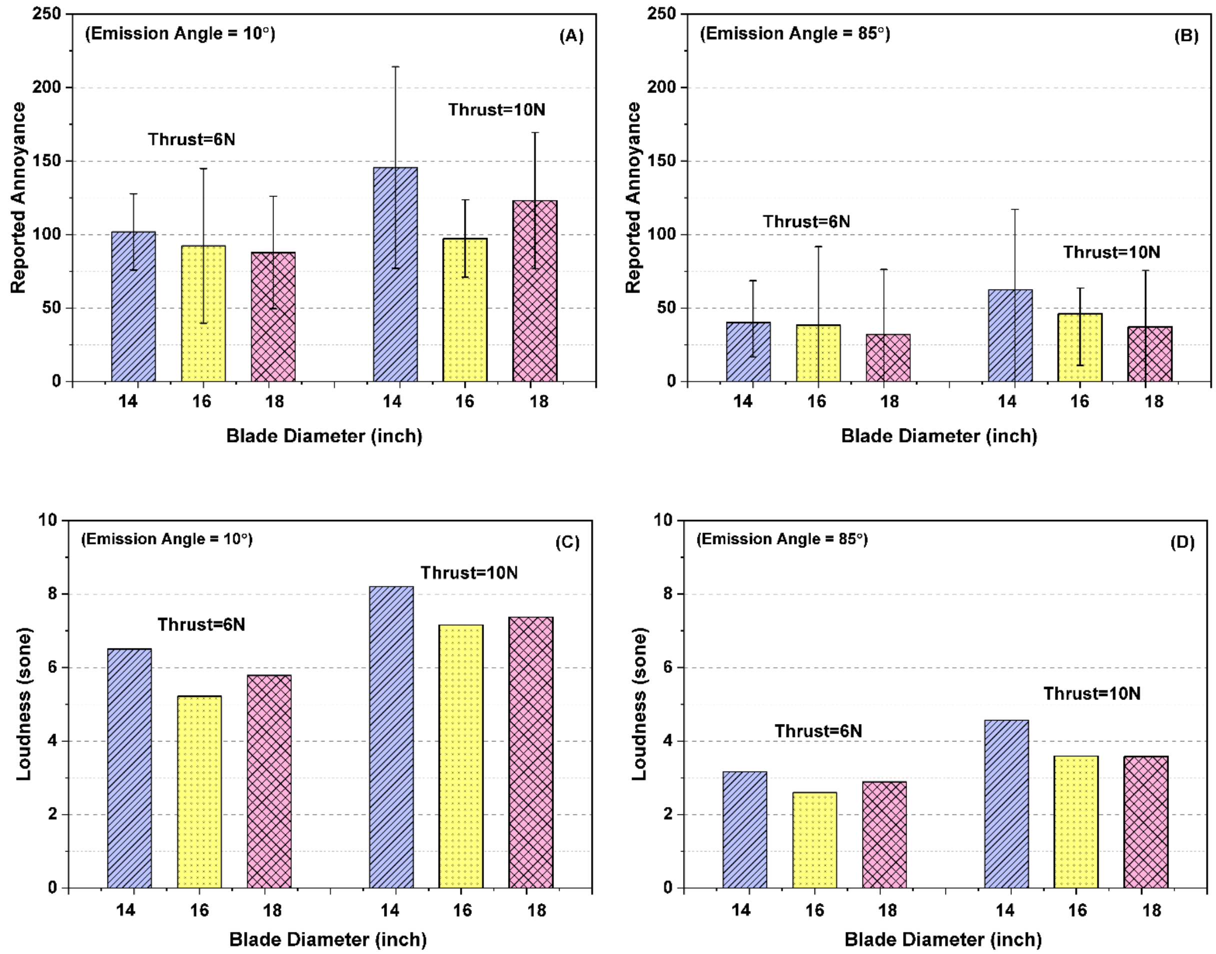

Figure 5. Reported annoyance (inter-individual average value) (A and B) and Loudness (C and D) as a function of blade diameter for the single rotor system. Data is displayed for 6 N and 10 N thrust settings and emission angles = 10 degrees (left) and 85 degrees (right). *Note that negative values in SD bars are due to reported data converted to a common master scale of annoyance (see section III.F) (color online)

Table II. Average values of Sharpness, Aures Tonality, Fluctuation Strength, Roughness and Impulsiveness as a function of blade diameter for the single rotor system. These average values include data for thrust settings of 6 N and 10 N, and for emission angles of 10 degrees and 85 degrees.

	Blade diameter = 14 in	Blade diameter = 16 in	Blade diameter = 18 in
Sharpness (acum)	2.72	2.60	2.60
Aures Tonality (tu)	0.45	0.48	0.35
Fluctuation Strength (vacil)	0.05	0.04	0.05
Roughness (asper)	0.66	0.70	0.80
Impulsiveness (iu)	0.10	0.16	0.23

Figure 6 shows the average values (for emission angles of 10 degrees and 85 degrees) of Loudness and reported annoyance (i.e., inter-individual average value) as a function of rotor-rotor axial spacing, for the three combinations of blade diameters in the contra-rotating system (i.e., 14-14 in, 16-16 in and 18-18 in). As for the case of the single rotor system, an important reduction in Loudness, and consequently on reported annoyance, is found when the blade diameter increases from 14-14 in to 16-16/18-18 in. Also, as for the grouped analysis presented in Section IV. B, the axial spacing between rotors leading to the lowest values of Loudness and reported annoyance is $z/D = 0.2$. This has been found for the three combinations of blade diameters investigated, except for the reported annoyance for the 14-14 in blade diameter. In this case, the minimum value of reported annoyance is found at $z/D = 0.1$. Exploring the values of the other SQMs, an unusually high value of impulsiveness has been found for this combination of blade diameter at the axial spacing $z/D = 0.2$, which might have influenced the participants' responses (note that this is an assumption that needs further investigation, due to the confounding effect of Loudness in the association between Impulsiveness and reported annoyance). Although this experimental research was carried out for small diameter (low Reynolds number) rotor blades, impulsiveness has been found to notably contribute to the noise annoyance caused by helicopter rotor blades (i.e., high Reynolds number) (McMullen, 2014)). This seems to suggest that impulsiveness might be an important psychoacoustic feature to address noise annoyance of new rotorcraft vehicles (e.g., VTOL vehicles).

It should be noted that due to some issues with the presentation of certain stimuli to the participants (i.e., z/D = 0.05, 0.6 and 1.0 with 16-16 in blade diameter, and z/D = 0.1 and 0.2 with 18-18 in blade diameter), the values displayed for these stimuli in Figure 6 are predicted using the PA model presented in Section IV. D, rather than directly taken from participants' responses. However, as seen in the Figure 6, there is a substantial agreement in the trend between predicted and observed values of annoyance.

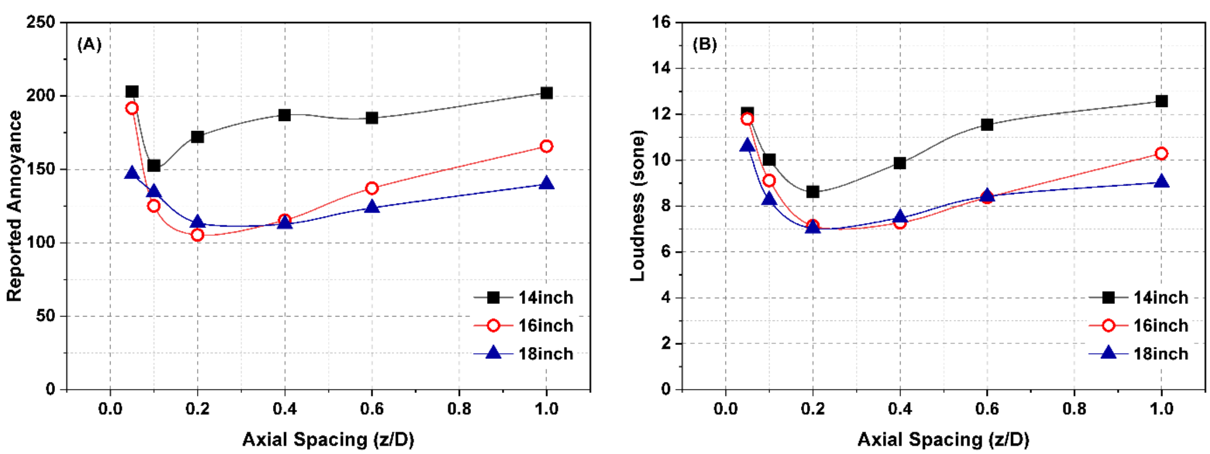

Figure 6. Loudness (A) and reported annoyance (inter-individual average values) (B) as a function of rotor-rotor axial spacing for the three blade diameters considered (14-14 in, 16-16 in and 18-18 in) for the contra-rotating system. Data is displayed is the average value of the emission angles 10

degrees and 85 degrees for thrust setting = 16 N. *Note that the unfilled triangles are predicted values using the PA model presented in Section IV. D. (color online)

D. Psychoacoustic annoyance model for rotor noise

Results in the previous sections IV. B and C suggest that the annoyance reported by the participants of this subjective experiment was mainly driven by Loudness. To investigate the contribution of each SQM to the noise annoyance reported for the different rotor noise stimuli, a partial correlation analysis was performed. Table III shows the zero-order (i.e., correlation between variables without controlling for any variable) and partial correlation (when controlling for Loudness) coefficients between the SQMs Sharpness, Aures Tonality, Roughness, Fluctuation Strength and Impulsiveness, and the reported annoyance. Without controlling for Loudness, Sharpness has a substantial negative correlation with annoyance; and Roughness and Fluctuation Strength have a substantial positive correlation with annoyance. However, when controlling for Loudness: (i) as expected, the correlation coefficients for all SQMs decreases, and (ii) Sharpness, Roughness and Impulsiveness have positive correlation coefficients with annoyance. In order words, when controlling for Loudness, an increase in the value of Sharpness, Roughness and Impulsiveness leads to an increase in the reported annoyance. This confirms that the association between the SQMs Sharpness, Aures Tonality, Roughness, Fluctuation Strength and Impulsiveness, and reported annoyance is influenced by Loudness as a confounding factor. Note that interdependencies between Loudness and the remaining SQMs is only for the description of the relationships with reported annoyance, and not between the SQMs and the main design parameters in the rotary systems investigated (which is the main topic of investigation in sections IV.A-C).

Table III. Zero-order and partial correlation coefficients (controlling for Loudness) between the SQMs Sharpness, Aures Tonality, Roughness, Fluctuation Strength and Impulsiveness, and the reported annoyance.

	Sharpness	Aures Tonality	Roughness	Fluctuation Strength	Impulsiveness
Zero-Order	-0.77*	0.11	0.77*	0.78*	-0.29*
Controlling for Loudness	0.21	-0.29*	0.30*	-0.43*	0.24*

*Statistically significant (< 0.05)

As pointed out above, some authors(Krishnamurthy *et al.*, 2018; Torija *et al.*, 2021) suggest that Impulsiveness and Roughness are likely to account for the perceptual response to propeller-turbulence interaction noise in rotary systems. None of the existing PA models include Impulsiveness in their formulation. Zwicker PA model (Zwicker and Fastl, 2013) accounts for the relationship between annoyance and Loudness, Sharpness, Fluctuation Strength and Roughness. Di et al. (Di *et al.*, 2016) and More (More, 2011) developed tonality factors to increase the accuracy of PA models for mechanical sounds in general and aircraft noise respectively.

A non-linear regression analysis was performed in IBM SPSS to derive an Impulsiveness factor, following the same approach of Zwicker PA model (Zwicker and Fastl, 2013) to derive the factor for Roughness. The normalised annoyance (0-1 interval) was set as dependent variable, and the Impulsiveness (I) and Loudness (N) were set at independent variables. The w_I factor is described in Equation 3:

$$w_I = \frac{0.075 \cdot I}{N^{-1.334}} \quad \text{(Equation 3)}$$

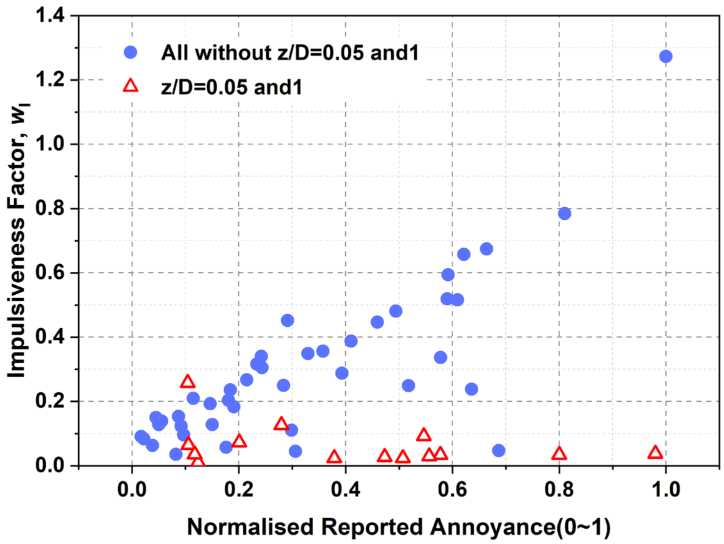

Figure 7. Impulsiveness factor (w_I) vs. reported annoyance (normalised to 0-1 interval) for all the configurations but axial spacings z/D = 0.05 and 0.1, and only axial spacings z/D = 0.05 and 0.1. (color online)

Figure 7 displays a dispersion diagram between the Impulsiveness factor w_I and the reported annoyance. For rotor-rotor axial spacings z/D = 0.05 and 0.1 (closest axial spacings), the reported annoyance is independent from the value of the Impulsiveness factor w_I. For all the other cases, i.e., excluding the axial spacings z/D = 0.05 and 0.1, there is a substantial correlation between the Impulsiveness factor w_I and the reported annoyance (R^2 = 0.76). The R^2 coefficient between the Impulsiveness factor w_I and the reported annoyance for all the configurations is 0.25. These results are consistent with the relationship between Impulsiveness and axial spacing in contra-rotating systems (see Figure 3 (F)). Although Loudness is the primary factor driving participants responses of annoyance for the rotary systems investigated in this research, the Impulsiveness factor (w_I) derived here can ensure a good prediction of noise annoyance caused by unsteady turbulence in rotary systems. A curve fitting procedure, with the data gathered in the subjective experiment, was used to formulated a new PA model for rotor noise (hereinafter referred to as 'Torija et al. PA model'). This model is described in Equation 4.

$$PA = N_5\left(1 + \sqrt{\gamma_0 + \gamma_1 w_S^2 + \gamma_2 w_{FR}^2 + \gamma_3 w_T^2 + \gamma_4 w_I^2}\right) \qquad \text{(Equation 4)}$$

where:

N_5 is the 5th percentile of the Loudness metric, w_S^2 and w_{FR}^2 are the factors for Sharpness and Roughness/Fluctuation Strength developed by Zwicker (Zwicker and Fastl, 2013), w_T^2 is the Tonality factor developed by More (More, 2011), and w_I^2 is the Impulsiveness factor presented above. Note that the 5th percentile values of the SQMs have been used to compute all the factors in the PA model. The gamma coefficients in Equation 4 were calculated using a non-linear regression analysis with the reported annoyance as dependent variable and the different factors in Equation 4 as independent variables. The value of these gamma coefficients are: γ_0 = 103.08, γ_1 = 339.49, γ_2 = 121.88, γ_3 = 77.20 and γ_4 = 29.29.

Figure 8 shows the dispersion diagram between the reported annoyance (i.e., inter-individual average value per test sound) and the annoyance estimated with the PA models: Zwicker (Zwicker and Fastl, 2013), Di et al. (Di *et al.*, 2016), More (More, 2011) and Torija et al. (described in Equation 4). As it can be seen, there is a very good agreement between the reported and values of annoyance estimated with all the PA models. The R^2 values for the estimations with each PA model are (including all test sounds): 0.89 (Di et al.), 0.93 (Zwicker and More) and 0.94 (Torija et al.). The Mean Squared Errors (MSE) of each PA model are: $6.28 \cdot 10^{-3}$ (Di et al.), $4.45 \cdot 10^{-3}$ (More), $4.38 \cdot 10^{-3}$ (Zwicker) and

$3.92 \cdot 10^{-3}$ (Torija et al.). The achievement of good predictions of annoyance seems to confirm that, in general, the primary factor driving participants' responses (in this experiment and with these rotor noise stimuli) is Loudness.

Table IV shows the R^2 and MSE values of each PA model for both single rotor and contra-rotating test sounds. All the PA models evaluated allow a very good estimation of the reported annoyance, for both the single rotor and contra-rotating test sounds. The performance of the PA models is slightly worse for the contra-rotating test sounds, which might be due to the perceptual effect of more complex phenomena such as potential field interaction tones, beating effects between rotors and turbulence due to interaction effects. For all the cases evaluated, the PA model formulated and presented in this paper (i.e., Torija et al. PA model) achieves slightly better estimations that the other PA models considered. However, the improvement in performance is not significant, as the reported annoyance seems to be mainly driven by loudness (as described above).

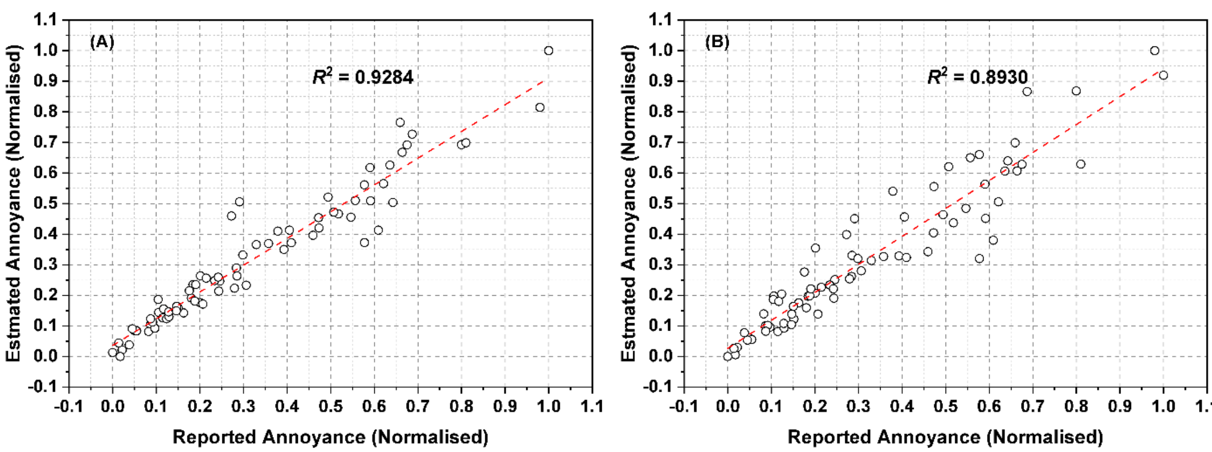

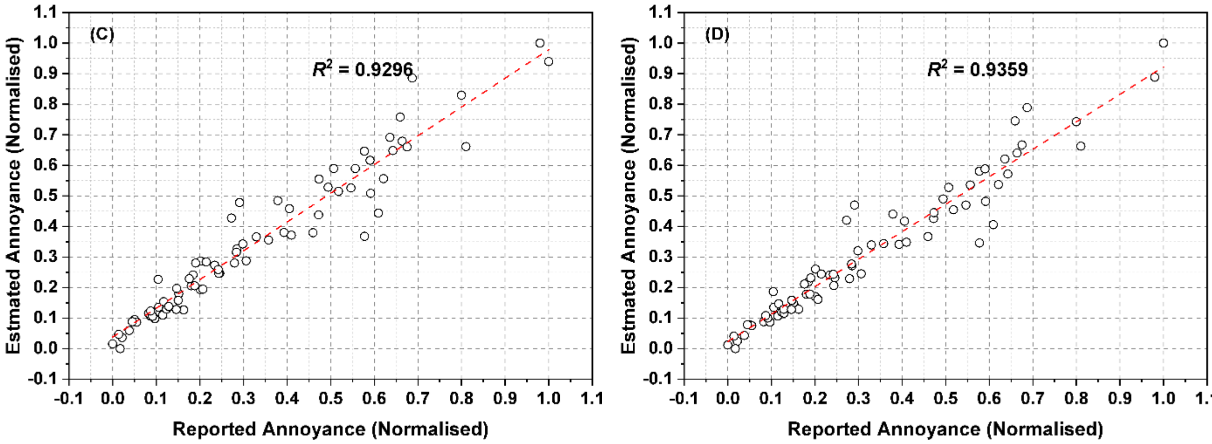

Figure 8. Reported annoyance (i.e., inter-individual average value per test sound) vs. estimated annoyance with the PA models: Zwicker (A), Di et al. (B), More (C) and Torija et al. (D) (formulated in this work). Note that the values of both reported and estimated annoyance are normalised to a 0-1 interval. (color online)

Table IV. R^2 and Mean Squared Error (MSE) values between the reported annoyance and the annoyance estimated with Zwicker's, Di et al.', More's PA models, and Torija et al. PA models.

	Single rotor		Contra-rotating	
	R^2	MSE	R^2	MSE
Zwicker PA model	0.929	$7.29 \cdot 10^{-4}$	0.917	$5.07 \cdot 10^{-3}$
Di et al. PA model	0.900	$1.35 \cdot 10^{-3}$	0.877	$7.20 \cdot 10^{-3}$
More PA model	0.940	$6.73 \cdot 10^{-4}$	0.917	$5.17 \cdot 10^{-3}$
Torija et al. PA model	0.944	$6.39 \cdot 10^{-4}$	0.925	$4.54 \cdot 10^{-3}$

The curve fitting model formulated in this paper can, however, be very useful to estimate rotor noise annoyance when loudness is not the dominant factor, or at least, other psychoacoustic factors are as important as loudness. This might be the case of contra-rotating systems with large rotor-rotor axial distance, where unsteadiness due to turbulence-propeller interaction leads to high values of impulsiveness (see Fig. 3 (F)). For the particular case of axial spacings (z/D) from 0.2 to 1.0 and an emission angle of 85 degrees (lowest emission of potential field interaction tones), the MSE value of the Torija et al. PA model ($4.98 \cdot 10^{-4}$) is at least half the MSE value of the other three PA models considered: $7.40 \cdot 10^{-4}$(Di et al.), $7.64 \cdot 10^{-4}$ (Zwicker) and $1.40 \cdot 10^{-3}$ (More). Of course, further investigation is required to quantify the applicability and overall performance of the curve fitting PA model for the wider range of configurations in rotary systems.

V. CONCLUSION

This paper presents the results of a psychoacoustic analysis of a comprehensive database of rotor noise samples encompassing different blade geometries, thrust settings, emissions angles, and single vs. contra-rotating propellers. The results of a listening experiment suggest that the reported annoyance of the rotor sounds evaluated was highly linked to the perceived loudness. Other psychoacoustic factors such as tonality content and high frequency content, low frequency amplitude modulation due to beating effects between rotors, and perceived roughness and impulsiveness due to turbulence caused by interaction effects were analysed and discussed as important contributors to the reported annoyance for the different rotor configurations studied. As a result of the research carried out, a psychoacoustic annoyance model has been formulated and analysed. A curve fitting procedure has been carried out to account for the major psychoacoustic factors influencing rotor noise annoyance investigated in this research. An important contribution is the development of a psychoacoustic function to account for the perceptual effects of impulsiveness. Impulsiveness seems to be an important factor to be considered in the assessment of noise annoyance of new rotorcraft vehicles, including multiple rotors configurations and VTOL transition maneuvers.

Further research is needed to encompass more configurations and operating conditions where the perceived loudness is not the main driving factor for annoyance. This research will help to better understand the perceptual effects of other relevant psychoacoustic factors on rotor noise annoyance.

ACKNOWLEGEMENTS

A.J.T. would like to acknowledge the funding provided by Innovate UK and the UK Aerospace Technology Institute (Project number: 73692). P.C. would like to acknowledge the financial support of the Royal Academy of Engineering, United Kingdom (RF/201819/18/194). The authors would also like to thank Dr. Mantas Brazinskas and Dr. Stephen Prior for their efforts in building this rig at the University of Southampton. Z.L. would like to acknowledge the funding from the Natural Science Foundation of Zhejiang University of Science and Technology (No. 2019QN15) and the funding from General Research Project of Zhejiang Provincial Department of Education (No. Y201839836).

REFERENCES

Berglund, M. B. (**2013**). ". Quality Assurance in Environmental Psychophysics," in *Ratio scaling of psychological magnitude* (Psychology Press), pp. 156-178.

Boucher, M., Krishnamurthy, S., Christian, A., and Rizzi, S. A. "Sound quality metric indicators of rotorcraft noise annoyance using multilevel regression analysis," (ASA).

Boucher, M., Krishnamurthy, S., Christian, A., and Rizzi, S. A. (**2019**). "Sound quality metric indicators of rotorcraft noise annoyance using multilevel regression analysis," in *Proceedings of Meetings on Acoustics 177ASA* (Acoustical Society of America), p. 040004.

Brazinskas, M., Prior, S., and Scanlan, J. (**2016**). "An Empirical Study of Overlapping Rotor Interference for a Small Unmanned Aircraft Propulsion System," Aerospace **3**, 32.

Brentner, K. S., and Farassat, F. (**1994**). "Helicopter Noise Prediction: The Current Status and Future Direction," Journal of Sound and Vibration **170**, 79-96.

Brès, G. A., Brentner, K. S., Perez, G., and Jones, H. E. (**2004**). "Maneuvering rotorcraft noise prediction," Journal of Sound and Vibration **275**, 719-738.

De Coensel, B., Botteldooren, D., Berglund, B., Nilsson, M. E., De Muer, T., and Lercher, P. (**2007**). "Experimental investigation of noise annoyance caused by high-speed trains," Acta acustica united with acustica **93**, 589-601.

Di, G.-Q., Chen, X.-W., Song, K., Zhou, B., and Pei, C.-M. (**2016**). "Improvement of Zwicker's psychoacoustic annoyance model aiming at tonal noises," Applied Acoustics **105**, 164-170.

Fields, J. M., and Powell, C. A. (**1987**). "Community reactions to helicopter noise: Results from an experimental study," The Journal of the Acoustical Society of America **82**, 479-492.

Gjestland, T. (**1994**). "Assessment of Helicopter Noise Annoyance: a Comparison Between Noise from Helicopters and from Jet Aircraft," Journal of Sound and Vibration **171**, 453-458.

Gojon, R., Jardin, T., and Parisot-Dupuis, H. (**2021**). "Experimental investigation of low Reynolds number rotor noise," The Journal of the Acoustical Society of America **149**, 3813-3829.

Gwak, D. Y., Han, D., and Lee, S. (**2020**). "Sound quality factors influencing annoyance from hovering UAV," Journal of Sound and Vibration, 115651.

Huang, Y., and Griffin, M. J. (**2014**). "Comparison of absolute magnitude estimation and relative magnitude estimation for judging the subjective intensity of noise and vibration," Applied Acoustics **77**, 82-88.

Intaratep, N., Alexander, W. N., Devenport, W. J., Grace, S. M., and Dropkin, A. (**2016**). "Experimental study of quadcopter acoustics and performance at static thrust conditions," in *22nd AIAA/CEAS Aeroacoustics Conference*, p. 2873.

Krishnamurthy, S., Christian, A., and Rizzi, S. (**2018**). "Psychoacoustic Test to Determine Sound Quality Metric Indicators of Rotorcraft Noise Annoyance," INTER-NOISE and NOISE-CON Congress and Conference Proceedings **258**, 317-328.

Luan, H., Weng, L., Liu, R., Li, D., and Wang, M. (**2019**). "Axial Spacing Effects on Rotor-Rotor Interaction Noise and Vibration in a Contra-Rotating Fan," International Journal of Aerospace Engineering **2019**, 2125976.

McKay, R., Kingan, M., and Go, S. T. (**2019**). *Experimental investigation of contra-rotating multi-rotor UAV propeller noise*.

McMullen, A. L. (**2014**). "Assessment of noise metrics for application to rotorcraft," (Purdue University).

More, S. (**2011**). "Aircraft noise metrics and characteristics," PARTNER Project 24 Report COE-2011 **4**.

Paruchuri, C. C., Joseph, P., Akiwate, D. C., Parry, A. B., and Prior, S. D. (**2021**). "On the noise generation mechanisms of overlapping propellers," in *AIAA AVIATION 2021 FORUM*, p. 2281.

Romani, G., and Casalino, D. (**2019**). "Rotorcraft blade-vortex interaction noise prediction using the Lattice-Boltzmann method," Aerospace Science and Technology **88**, 147-157.

Stallen, P. J. (**1999**). "A theoretical framework for environmental noise annoyance," Noise and Health **1**, 69-79.

Tinney, C. E., and Sirohi, J. (**2018**). "Multirotor Drone Noise at Static Thrust," AIAA Journal **56**, 2816-2826.

Torija, A. J., Chaitanya, P., and Li, Z. (**2021**). "Psychoacoustic analysis of contra-rotating propeller noise for unmanned aerial vehicles," The Journal of the Acoustical Society of America **149**, 835-846.

Torija, A. J., and Clark, C. (**2021**). "A Psychoacoustic Approach to Building Knowledge about Human Response to Noise of Unmanned Aerial Vehicles," International Journal of Environmental Research and Public Health **18**, 682.

Torija, A. J., and Flindell, I. H. (**2015**). "The subjective effect of low frequency content in road traffic noise," The Journal of the Acoustical Society of America **137**, 189-198.

Torija, A. J. S., Rod H.; Lawrence, Jack L.T. (**2019**). "Psychoacoustic Characterisation of a Small Fixed-pitch Quadcopter," in *INTER-NOISE and NOISE-CON Congress and Conference Proceedings, InterNoise19* (Institute of Noise Control Engineering, Madrid, Spain), pp. 1884-1894(1811).

Whelchel, J., Alexander, W. N., and Intaratep, N. (**2020**). "Propeller noise in confined anechoic and open environments," in *AIAA Scitech 2020 Forum*, p. 1252.

Zawodny, N. S., and Boyd, D. D. (**2019**). "Investigation of Rotor-Airframe Interaction Noise Associated with Small-Scale Rotary-Wing Unmanned Aircraft Systems," Journal of The American Helicopter Society **65**, 1-17.

Zawodny, N. S., Boyd, D. D., and Burley, C. (**2016**). "Acoustic Characterization and Prediction of Representative, Small-Scale Rotary-Wing Unmanned Aircraft System Components."

Zwicker, E., and Fastl, H. (**2013**). *Psychoacoustics: Facts and models* (Springer Science & Business Media).